

Computation of invariant tori and whiskers in quasiperiodically forced systems

Theory, algorithms, numerical explorations, conjectures

Àlex Haro

Departament de Matemàtica Aplicada i Anàlisi
Universitat de Barcelona

IMA (University of Minnesota), June 2011

Preface

Robust landmarks

2

The long term behaviour of a dynamical system is organized by its invariant objects.

Hence, it is important to:

- understand which invariant objects persist under perturbations of the system;
- provide results about their existence, regularity and dependence with respect to parameters;
- classify their bifurcations and mechanisms of breakdown.

These robust objects are **normally hyperbolic invariant manifolds** (NHIM).

Preface

3

In this lecture ...

We address these questions for a class of dynamical systems and invariant objects: **quasiperiodic forced systems** and **Fiberwise Hyperbolic Invariant Tori (FHIT)**.

Skew product systems modelize systems driven by another.

The invariant tori we consider are the response to the quasiperiodic forcing.

Theorems

Quasiperiodically forced systems

5

Mathematical model

A **quasi-periodic map** with irrational frequency vector $\omega \in \mathbb{R}^d$ is a skew product in $\mathbb{R}^n \times \mathbb{T}^d$

$$\begin{cases} \bar{x} = F(x, \theta) \\ \bar{\theta} = \theta + \omega \pmod{1} \end{cases},$$

where $F : \mathbb{R}^n \times \mathbb{T}^d \rightarrow \mathbb{R}^n$.

We assume F of class C^{r+1} .

Quasiperiodically forced systems

Invariance equation for invariant tori

Given a quasi-periodic map

$$\begin{cases} \bar{x} = F(x, \theta) \\ \bar{\theta} = \theta + \omega \pmod{1} \end{cases},$$

a solution $K : \mathbb{T}^d \rightarrow \mathbb{R}^n$ of

$$F(K(\theta), \theta) = K(\theta + \omega), \quad (1)$$

parameterizes an **invariant torus**

$$\mathcal{K} = \{(K(\theta), \theta) \mid \theta \in \mathbb{T}^d\}$$

whose dynamics is a rotation.

This torus is a response to the quasiperiodic forcing.

Quasiperiodically forced systems

7

Invariance equation for (1-rank) whiskers

Given a quasi-periodic map

$$\begin{cases} \bar{x} = F(x, \theta) \\ \bar{\theta} = \theta + \omega \pmod{1} \end{cases},$$

A solution $W : \mathbb{T}^d \times \mathbb{R} \rightarrow \mathbb{R}^n$, $\lambda \in \mathbb{R}$ of

$$F(W(\theta, \mathbf{s}), \theta) = W(\theta + \omega, \lambda \mathbf{s}), \quad (2)$$

parameterizes an **invariant manifold**

$$\mathcal{W} = \{(W(\theta, \mathbf{s}), \theta) \mid \theta \in \mathbb{T}^d, \mathbf{s} \in \mathbb{R}\}$$

whose dynamics is the product of a rotation and a homothety.

This is the simplest case. But theory works for higher rank whiskers.

Fiberwise hyperbolic invariant tori

8

Dynamical definition

A **FHIT** is a graph of a continuous map $K: \mathbb{T}^d \rightarrow \mathbb{R}^n$ such that:

- 1 **Invariance:** $K(\theta + \omega) = F(K(\theta), \theta)$, $\forall \theta \in \mathbb{T}$.
- 2 **Hyperbolicity:** The fiber bundle $\mathbb{R}^n \times \mathbb{T}^d$ decomposes in a continuous invariant Whitney sum $E^s \oplus E^u$ such that $D_z F|_{E^u}$ is invertible and there exist $0 < \lambda < 1$ and $C > 0$ for which
 - If $(v, \theta) \in E^s$ and $m > 0$, then

$$\|D_z F^m(K(\theta), \theta)v\| < C\lambda^m \|v\|.$$

- If $(v, \theta) \in E^u$ and $m < 0$, then

$$\|D_z F^m(K(\theta), \theta)v\| < C\lambda^{-m} \|v\|.$$

Fiberwise hyperbolic invariant tori

Functional definition

A **FHIT** is a graph of a continuous map $K: \mathbb{T}^d \rightarrow \mathbb{R}^n$ such that:

- 1 **Invariance:** K is a fixed point of

$$\mathcal{F}: \begin{array}{ccc} \mathcal{C}^0(\mathbb{T}^d, \mathbb{R}^n) & \longrightarrow & \mathcal{C}^0(\mathbb{T}^d, \mathbb{R}^n) \\ K & \longrightarrow & F(K(\theta - \omega), \theta - \omega) \end{array} .$$

- 2 **Hyperbolicity:** The transfer operator

$$D\mathcal{F}: \begin{array}{ccc} \mathcal{C}^0(\mathbb{T}^d, \mathbb{R}^n) & \longrightarrow & \mathcal{C}^0(\mathbb{T}^d, \mathbb{R}^n) \\ \sigma & \longrightarrow & D_z F(K(\theta - \omega), \theta - \omega) \sigma(\theta - \omega) \end{array} .$$

is hyperbolic, i.e. its (Mather) spectrum does not intersect the unit circle.

Interlude: Spectral Theory

10

Cocycles and transfer operators

A **linear skew product** (cocycle) in \mathbb{R}^n over \mathbb{T}^d ,

$$\begin{cases} \bar{v} = M(\theta)v \\ \bar{\theta} = \theta + \omega \end{cases} ; \quad (3)$$

induces a **transfer operator** \mathcal{M}_ω acting on (bounded, continuous, C^r) sections $v : \mathbb{T}^d \rightarrow \mathbb{C}^n$ by

$$\mathcal{M}_\omega v(\theta) = M(\theta - \omega)v(\theta - \omega) . \quad (4)$$

*The **functional analysis** properties (4) are closely related to the **dynamical properties** of (3).*

Mather, Sacker, Sell, Palmer, Hirsch, Pugh, Shub, Mañé, Chicone, Swanson, Johnson, Latushkin, Stëpin, de la Llave, ...

Interlude: Spectral Theory

11

Properties of the spectrum

- The spectrum of \mathcal{M}_ω is a finite union of **spectral annuli**.
- Each spectral annulus induces an **invariant subbundle** of the cocycle M , characterized by **rates of growth**.
- If \mathcal{M}_ω is **hyperbolic**, the cocycle M has **stable/unstable subbundles**.
- **The spectrum is independent of the space of sections!**
[A.H., de la Llave] (for rotational dynamics in the base)

Example: if $n = 2$, the spectrum can be:

- Two circles of radii $\Lambda_1 < \Lambda_2$;
- One annulus of radii $\Lambda_1 < \Lambda_2$;
- One single circle of radius Λ .

The Λ 's are the **Lyapunov multipliers**.

Fiberwise hyperbolic invariant tori

12

Existence and persistence result

Theorem

Let F be C^{r+1} and K be C^r . Assume:

- K is an *approximate solution* of (1):

$$\|F(K(\theta - \omega), \theta - \omega) - K(\theta)\|_{C^r} \leq \varepsilon .$$

- Its *transfer operator* \mathcal{M}_ω on $B(\mathbb{T}^d, \mathbb{R}^n)$ is *hyperbolic*.

Then, if ε is small enough:

- 1 There exists an invariant graph K_F , and $\|K - K_F\|_{C^r} \leq c\varepsilon$.
- 2 The map $F \rightarrow K_F$ is C^1 from C^{r+1} to C^r .
- 3 The torus K_F is C^{r+1} (bootstrap of the differentiability).

Moreover, the torus K_F is *fiberwise hyperbolic*.

Asymptotic invariant manifolds

13

Existence result of (1 rank) whiskers

Theorem

Let F be C^{r+1} and K a C^r invariant torus. Let $\lambda \in \mathbb{R}$ be an eigenvalue of the transfer operator \mathcal{M}_ω acting in C^r , and $V : \mathbb{T}^d \rightarrow \mathbb{R}^n$ be its C^r -eigenfunction, i.e.

$$M(\theta)V(\theta) = \lambda V(\theta + \omega).$$

Assume that:

- $|\lambda| \neq 1$;
- For all $k \geq 2$, $\lambda^k \notin \text{Spec}(\mathcal{M}_\omega)$.

Then, if r is large enough, **there is a C^r invariant manifold tangent to the bundle of rank 1 generated by V** , whose dynamics is conjugate to the direct product of a rotation and an homothety.

Asymptotic invariant manifolds

14

Some remarks

- The theorem has a higher rank version, producing an invariant manifold associated to an invariant subbundle, under appropriate non-resonant conditions.
- Reducibility of normal dynamics is not an issue in this generalization.
- Even if the dynamics on the manifold could not be linearized, we can get that it is polynomial, whose coefficients depend on θ .
- One produces the classical **stable manifold** and **strong stable manifold**.
- One also produces smooth **slow manifolds** that are not available with the classical theory.
- One can obtain that **the manifolds are unique** under a suitable C^L regularity, depending only on spectral properties.

Algorithms

Invariant tori

Newton method

A Newton step is:

Given an approximate invariant torus K , with error

$$F(K(\theta - \omega), \theta - \omega) - K(\theta) = R(\theta) ,$$

the improved torus is $\hat{K} = K + \Delta$, where

$$M(\theta - \omega)\Delta(\theta - \omega) - \Delta(\theta) = -R(\theta) , \quad (5)$$

where $M(\theta) = DF(K(\theta), \theta)$.

Feasible Newton step in the same space if hyperbolicity holds.

Invariant tori

17

Computation

- The tori are expanded as Fourier series.
- If F is “simple”, the L.H.S. of the invariance equation (1)

$$F(K(\theta), \theta) = K(\theta + \omega),$$

is easily computed using **AD**. Otherwise, use **FT**.

- The Fourier discretization of the Newton-step (5)

$$M(\theta - \omega)\Delta(\theta - \omega) - \Delta(\theta) = -R(\theta)$$

produces **Large matrices!**

- If $M(\theta)$ is **reducible** to constants, i.e.

$$M(\theta)P(\theta) = P(\theta + \omega)\Lambda \tag{6}$$

for suitable $P(\theta)$ and Λ , then (5) is “diagonal” in the Fourier modes, producing **Fast computations!**

These observations are also useful in KAM theory [de la Llave et al].

See also [Castellà, Jorba 00], [Jorba, Olmedo 10].

Asymptotic invariant manifolds

18

Normal form method

To solve $F(W(\theta, s), \theta) = W(\theta + \omega, \lambda s)$, we expand W as

$$W(\theta, s) = W_0(\theta) + W_1(\theta)s + W_2(\theta)s^2 + \dots,$$

obtaining a **hierarchy** of equations:

$k = 0$) **Tori invariance eq.:** $F(W_0(\theta), \theta) = W_0(\theta + \omega)$,
so $W_0(\theta) = K(\theta)$.

$k = 1$) **Eigenvalue eq.:** $M(\theta)W_1(\theta) = \lambda W_1(\theta + \omega)$,
so $W_1(\theta) = V(\theta)$ is an eigenfunction of \mathcal{M}_ω .

$k \geq 2$) **Homological eq.:** $M(\theta)W_k(\theta) - \lambda^k W_k(\theta + \omega) = C_k(\theta)$,
where C_k depends on the previously computed terms.

Non-resonance condition: for $k \geq 2$, $\lambda^k \notin \text{Spec}(\mathcal{M}_\omega)$.

Asymptotic invariant manifolds

19

Computation of the expansions

- The whiskers are expanded as Fourier-Taylor series.
- If F is “simple”, the L.H.S. of the invariance equation (1)

$$F(W(\theta, s), \theta) = W(\theta + \omega, \lambda s) ,$$

is easily computed using **AD**. The R.H.S. is straightforward.

- The methods yields **high precision** results.
- Useful to **globalize** the manifold.

Numerical explorations in a dissipative system

The rotating Hénon map

21

A dissipative quasiperiodic system

$$\begin{cases} \bar{x} = 1 + y - a x^2 + \varepsilon \cos(2\pi\theta) \\ \bar{y} = bx \\ \bar{\theta} = \theta + \omega \pmod{1} \end{cases}$$

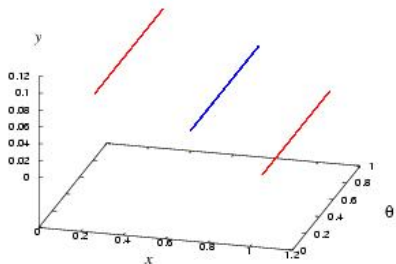
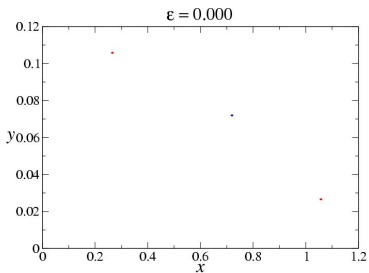
- a is the nonlinear parameter ($a = 0.68$);
- b is the dissipative parameter ($b = 0.1$);
- ε is the quasi-periodic parameter;
- $\omega = \frac{1}{2}(\sqrt{5} - 1)$ is the frequency of the forcing.

[Krauskopf,Osinga 98][Feudel,Osinga 00]

The rotating Hénon map

22

Invariant tori

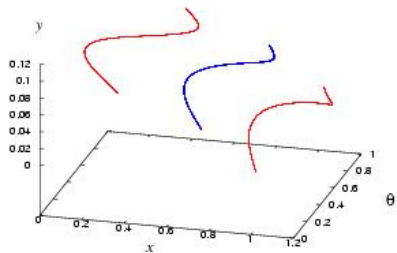
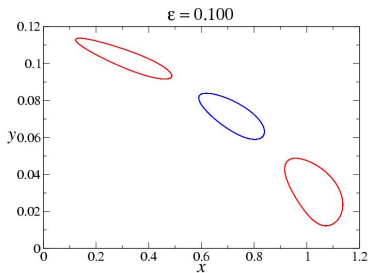


The saddle type **fixed point** and the stable **2 periodic orbit** of the Hénon map ...

The rotating Hénon map

23

Invariant tori

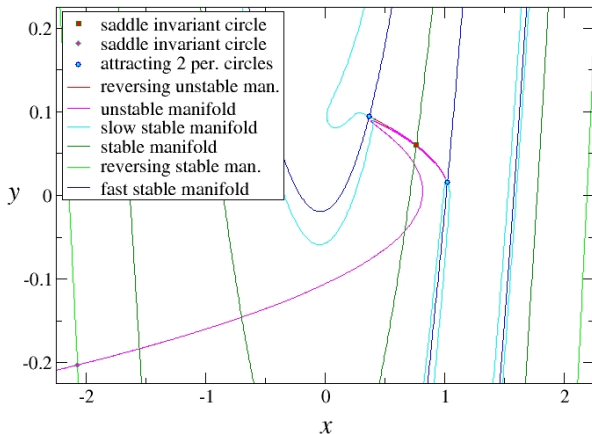


... turn into an **invariant circle** and a **2 periodic circle** for the RHM with $\varepsilon = 0.100$.

The rotating Hénon map

24

Invariant manifolds

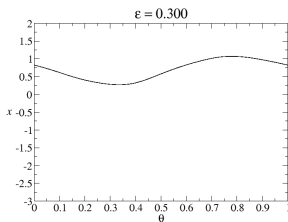
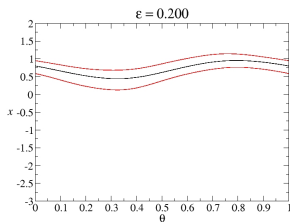
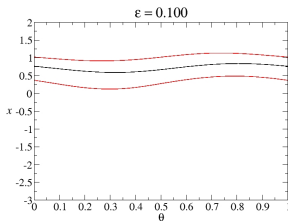
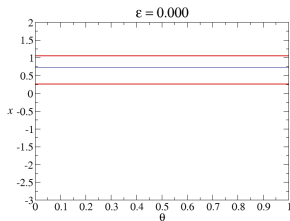


Sections with $\theta = 0$ of the invariant manifolds, for $\varepsilon = 0.1$.

Continuation of an invariant torus

25

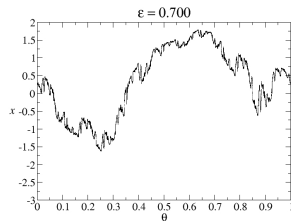
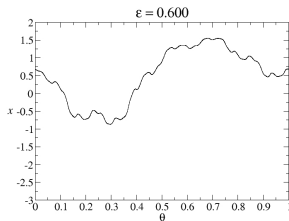
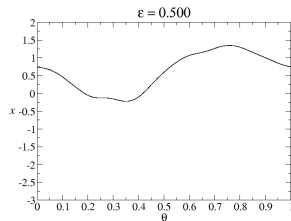
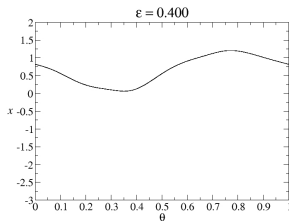
(I) Period “halving” (from saddle to attracting torus)



Continuation of an invariant torus

26

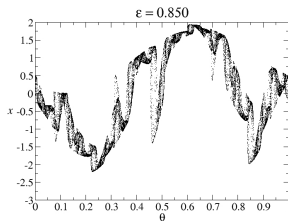
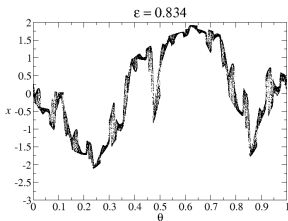
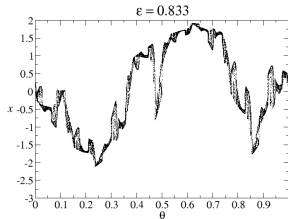
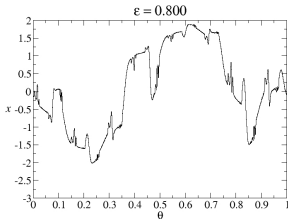
(II) Continuation of an attracting torus



Continuation of an invariant torus

27

(III) Fractalization of the torus



Continuation of a reducible invariant torus

28

An obstruction to reducibility

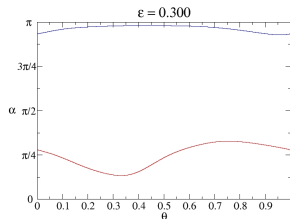
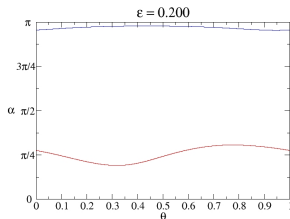
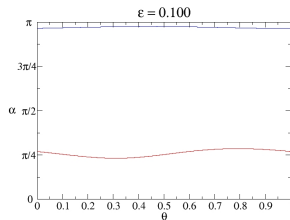
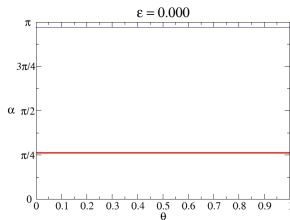
Rotating Hénon map: $a= 0.68$, $b= 0.1$

ε	eigenvalues	error	nfm
0.000	-1.0721039594 , 0.0932745366	9.6e-21	100
0.200	-1.0297559933 , 0.0971103841	8.3e-21	100
0.400	-0.8288693291 , 0.1206462786	9.6e-20	100
0.450	-0.6721643269 , 0.1487731437	9.9e-13	100
0.460	-0.6034304995 , 0.1657191675	2.9e-14	300
0.461	-0.5925812920 , 0.1687532181	2.7e-12	300
0.462	-0.5792054526 , 0.1726503084	2.3e-13	400
0.463	-0.5584521519 , 0.1790663706	9.1e-10	6800

Invariant directions (projectivized bundles)

29

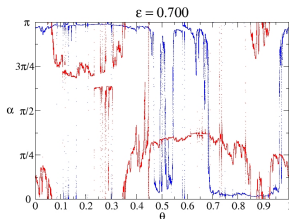
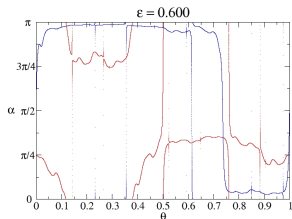
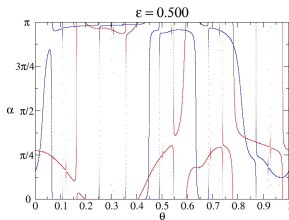
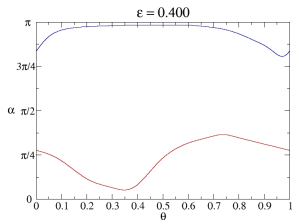
(I) Unstable direction becomes a slow stable direction



Invariant directions (projectivized bundles)

30

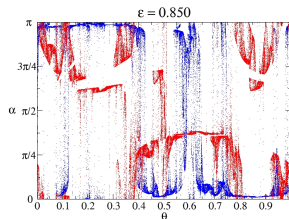
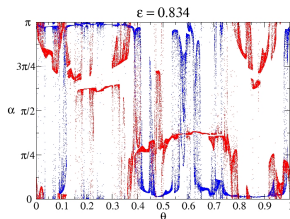
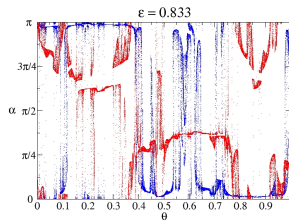
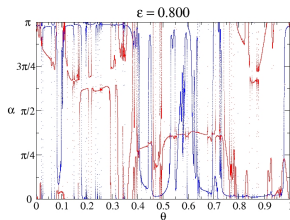
(II) Merging of invariant directions



Invariant directions (projectivized bundles)

31

(III) Invariant directions for the fractalization of the torus

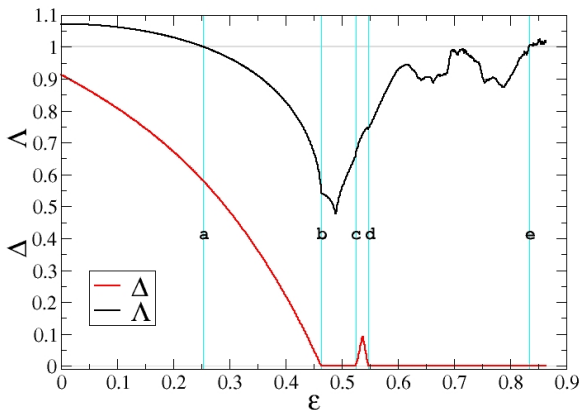


Description of the bifurcations

32

Observables: Λ (maximal Lyapunov multiplier)

Δ (distance between bundles)



a) **Period halving** bifurcation.

b, c, d) **Bundle merging** bifurcation, a global bifurcation.

The bundle merging bifurcation

33

Description and consequences

The invariant bundles approach each other while the Lyapunov multipliers $\Lambda_- < \Lambda_+$ remain different from 1.

- The **reducibility breaks down**.
- In spectral terms, as the parameter approaches the critical value
 - The **spectrum is two circles**, of radii $\Lambda_- < \Lambda_+$.
 - The distance of the two circles is bounded from below.
 - The norm of the spectral projections grows to infinity.

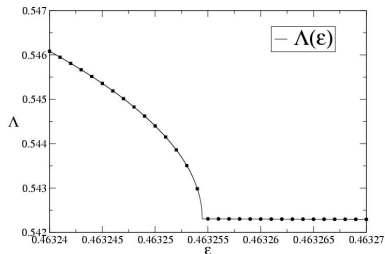
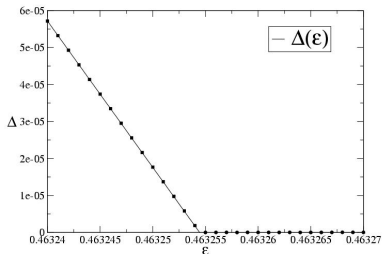
At the critical value, the **spectrum is a filled annulus**.

- The invariant bundles are not continuous when they collapse, but measurable [Oseledec68]. Their projectivizations are SNA (**Strange Nonchaotic Attractors**).

The bundle merging bifurcation

34

Quantitative estimates (universal laws)



$$\begin{cases} \Delta_\varepsilon \sim \alpha(\varepsilon_b - \varepsilon)^\beta & \text{if } \varepsilon \lesssim \varepsilon_b \\ \Delta_\varepsilon \approx 0 & \text{if } \varepsilon \gtrsim \varepsilon_b \end{cases}$$

$$\begin{cases} \Lambda_\varepsilon \sim \Lambda_b + A(\varepsilon_b - \varepsilon)^B & \text{if } \varepsilon \lesssim \varepsilon_b \\ \Lambda_\varepsilon \approx \Lambda_b + \bar{A}(\varepsilon - \varepsilon_b)^{\bar{B}} & \text{if } \varepsilon \gtrsim \varepsilon_b \end{cases}$$

$$\varepsilon_b = 0.46325447112$$

$$\alpha = 3.94933$$

$$\beta = 0.999979 \approx 1$$

$$\Lambda_b = 0.5423122$$

$$A = 1.015$$

$$B = 0.5020 \approx 0.5$$

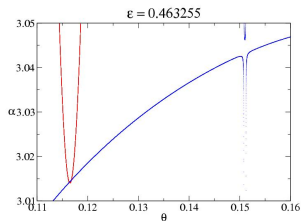
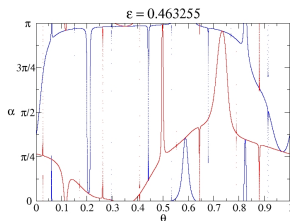
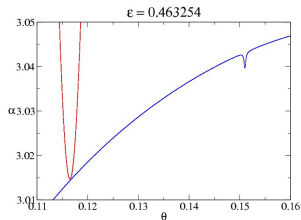
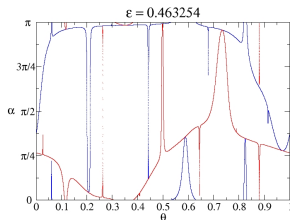
$$\bar{A} = -0.7409$$

$$\bar{B} = 1.00035 \approx 1$$

The bundle merging bifurcation

35

Visual verification of the collapse



Projectivization of the **slow** and **fast** stable bundles, and zooms.

The bundle merging bifurcation

36

An analytical justification of bundle collapse

- For $\varepsilon = 0.460$, the torus is attracting and the cocycle is reducible to a constant diagonal matrix

$$\text{diag}(-0.6034304995, 0.1657191675).$$

- For $\varepsilon = 0.530$, the torus is attracting and the cocycle is reducible to a constant diagonal matrix

$$\text{diag}(0.6945467500, -0.1439787890).$$

- Since the Lyapunov multipliers are different during the continuation,

the cocycle can not be reducible during the whole continuation!

The bundle merging bifurcation

37

Description and consequences

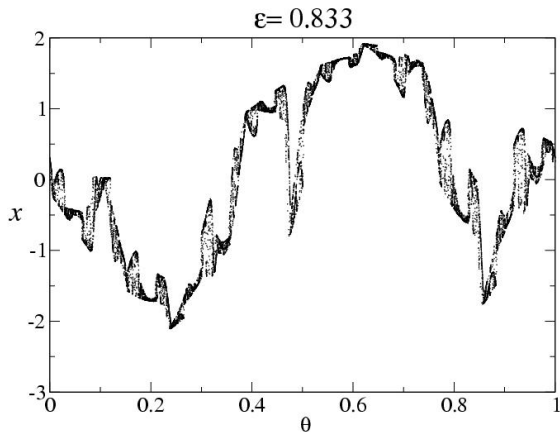
The invariant bundles approach each other when $\varepsilon < \varepsilon_c$, and collapse for $\varepsilon = \varepsilon_c$, while the Lyapunov multipliers $\Lambda_\varepsilon^- < \Lambda_\varepsilon^+$ remain different.

	$\varepsilon < \varepsilon_c$	$\varepsilon = \varepsilon_c$
Linear dynamics: Invariant bundles	Continuous	Measurable [Oseledets 68]
Projective dynamics: Invariant curves	Continuous (attracting / repelling)	Measurable (SNA / SNR)
Spectrum	Two circles of radii Λ_ε^\pm	Annulus of radii Λ_ε^\pm
Reducibility (ω Diophantine)	Yes	No
If $\Lambda_\varepsilon^- < \Lambda_\varepsilon^+ < 1$	Attracting torus	The torus survives
If $\Lambda_\varepsilon^- < 1 < \Lambda_\varepsilon^+$	Saddle torus	The torus is destroyed

After the bundle merging scenario

38

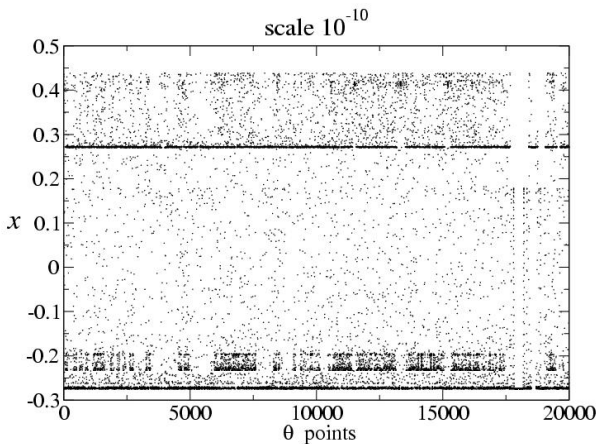
Zooms of the attractor (using multiprecision)



After the bundle merging scenario

39

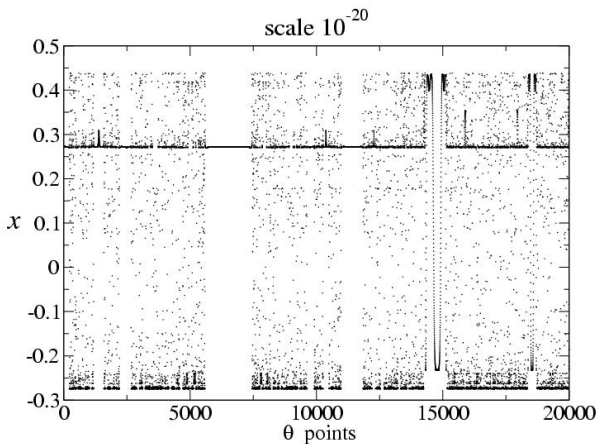
Zooms of the attractor (using multiprecision)



After the bundle merging scenario

40

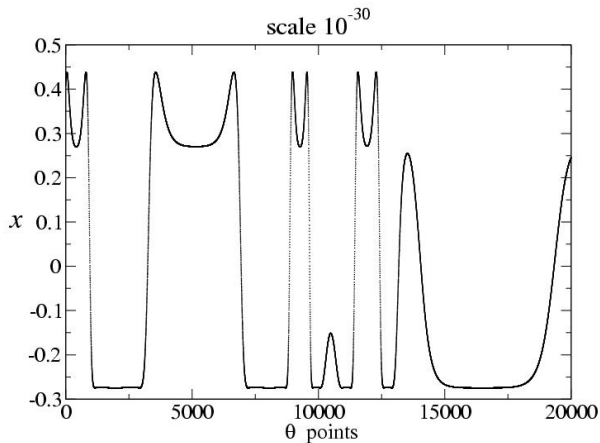
Zooms of the attractor (using multiprecision)



After the bundle merging scenario

41

Zooms of the attractor (using multiprecision)



From the numerical experiments

42

The formation of a SNA in the linearized dynamics of an attracting torus produces a sudden growth of the spectrum.

There are scaling relations in the observables (distance between bundles, Lyapunov multipliers), that are universal.

See [Bjerklöv, Saprykina 08] for some proofs.

The phenomenon is the prelude of the destruction of the torus in a fractalization route.

Conjecture: The torus is destroyed when the maximal Lyapunov multiplier crosses 1.

See [Figueras] (thesis) for a fractalization of a saddle torus in 3D.

Numerical explorations in a conservative system

The rotating standard map

$$\begin{cases} \bar{x} = x + \bar{y} \pmod{1} \\ \bar{y} = y - \frac{\sin(2\pi x)}{2\pi} (K + \varepsilon \cos(2\pi\theta)) \\ \bar{\theta} = \theta + \omega \pmod{1} \end{cases}$$

- K is the parameter of the standard map ($K = 0.2$);
- ε is the quasi-periodic parameter;
- ω is an algebraic number of order 3:

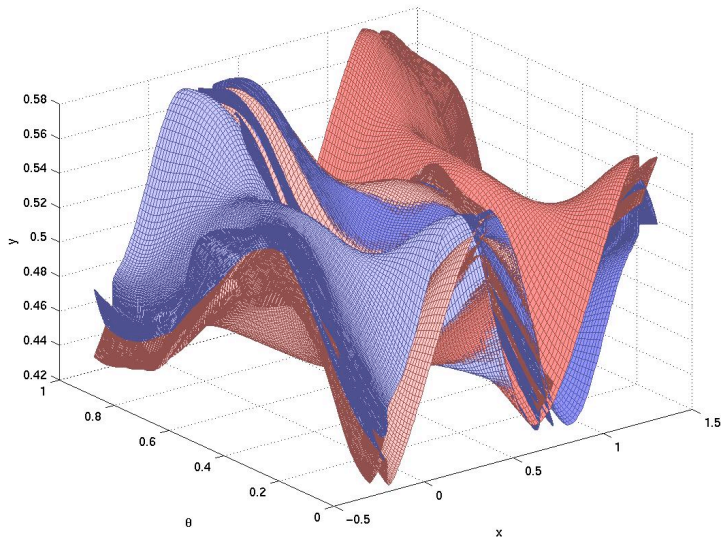
$$\omega = \sqrt[3]{\frac{19}{27} + \sqrt{\frac{11}{27}}} + \sqrt{\frac{11}{27}} + \sqrt[3]{\frac{19}{27} - \sqrt{\frac{11}{27}}} - \frac{2}{3}.$$

[Artuso et al 91, Tompaidis 96, Haro 98]

Invariant manifolds of a 2-periodic torus ($\varepsilon = 0.5$)

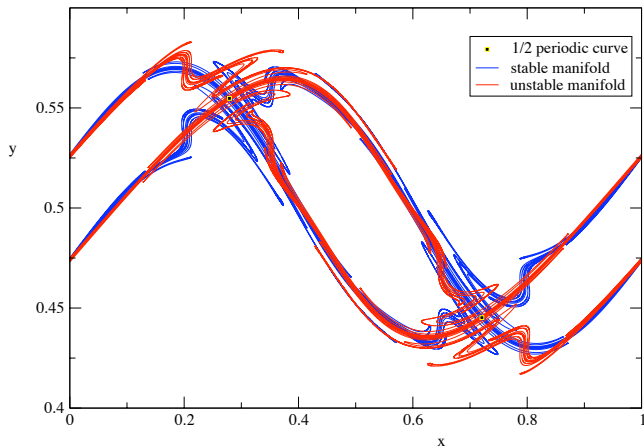
45

3D view



Invariant manifolds of a 2-periodic torus ($\varepsilon = 0.5$)

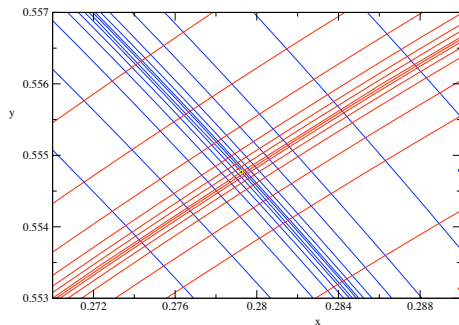
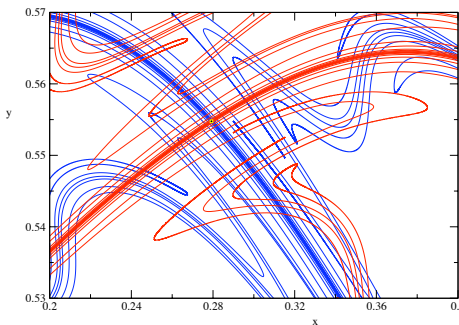
46

Slice $\theta = 0$ 

Invariant manifolds of a 2-periodic torus ($\varepsilon = 0.5$)

47

Zooms



Bifurcations at resonance

Continuation of an elliptic torus

Rotating standard map: $K = 0.2$. Torus $\{x = 0, y = 0\}$

ε	eigenvalues	error	nfm
0.010	$\exp(\pm 0.4513209919 \text{ i})$	1.6e-19	100
0.030	$\exp(\pm 0.4537325863 \text{ i})$	3.5e-19	100
0.050	$\exp(\pm 0.4589178272 \text{ i})$	2.1e-19	100
0.070	$\exp(\pm 0.4679895639 \text{ i})$	5.0e-19	100
0.090	$\exp(\pm 0.4857579944 \text{ i})$	8.4e-19	100
0.096	$\exp(\pm 0.5003407232 \text{ i})$	4.3e-18	100
0.09625	$\exp(\pm 0.5024691304 \text{ i})$	6.7e-18	100
ε_r	$\exp(\pm 0.5048955423 \text{ i})$	5.5e-10	450

Bifurcations at resonance

49

Detection of resonance

- For $\varepsilon = \varepsilon_r \simeq 0.09634888517236193761$
 - the **internal frequency** $\alpha \simeq 0.50489554233135677542$
 - the **external frequency** $\omega \simeq 0.83928675521416126683$

satisfy

$$\left| \frac{\alpha}{2\pi} - \frac{k_1 + k_2\omega}{2} \right| \simeq 1.1 \cdot 10^{-9},$$

for $k_1 = 1, k_2 = -1$.

- We improve reducibility using rotating transformations, so we can cross the resonance [Moser-Pöschel 86].
- After the bifurcations, the torus is hyperbolic. Moreover,
 - Since $k_1 = 1$ is odd, the eigenvalues are negative.
 - Since $k_2 = -1$ is odd, the invariant manifolds are non-orientable

Bifurcations at resonance

50

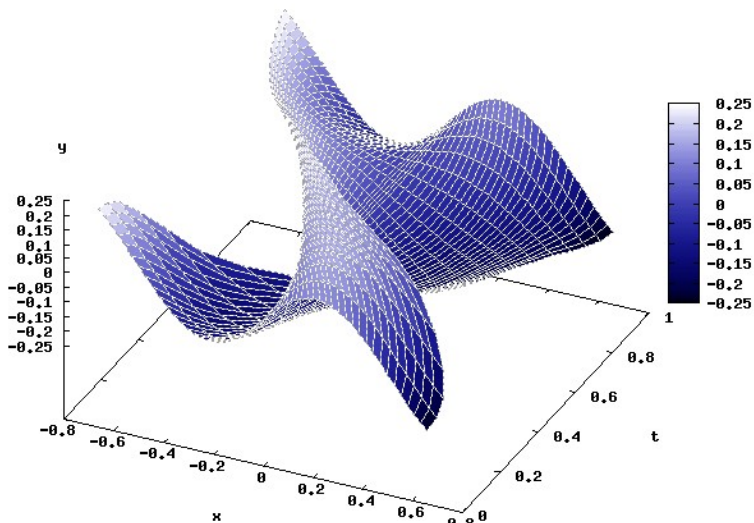
Crossing the resonance

Rotating standard map: $K = 0.2$. Torus $\{x = 0, y = 0\}$

ε	eigenvalues	error	nfm
0.010	$\exp(\pm 0.4513209918i)$	7.7e-20	100
0.030	$\exp(\pm 0.4537325863i)$	1.6e-19	100
0.050	$\exp(\pm 3.0956149315i)$	5.1e-10	100
0.070	$\exp(\pm 3.1046866683i)$	5.2e-19	100
0.090	$\exp(\pm 3.1224550988i)$	3.8e-19	100
0.100	-0.985229910 , -1.0149915151	3.0e-19	100
0.300	-0.859755912 , -1.1631208182	4.6e-19	100
0.500	-0.784499412 , -1.2746982141	3.7e-19	100

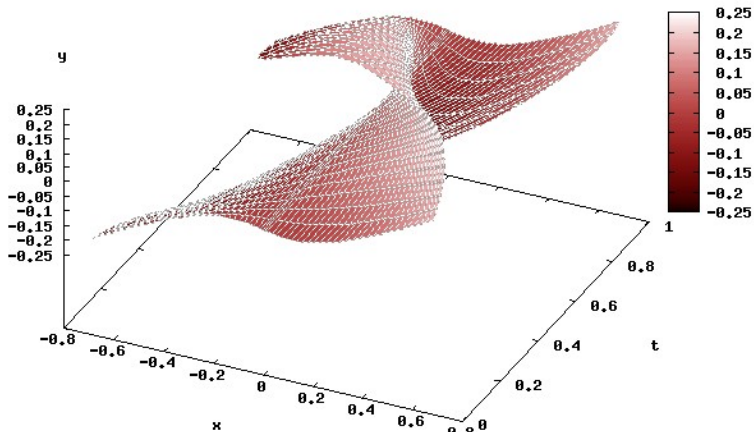
Non-orientable invariant manifolds

51

Stable manifold ($\varepsilon = 0.5$)

Non-orientable invariant manifolds

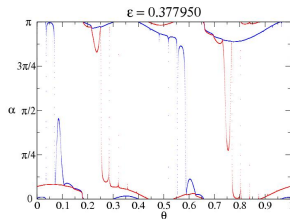
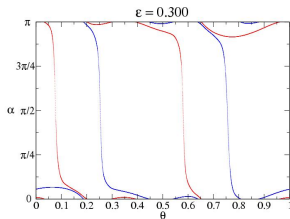
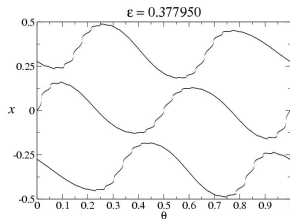
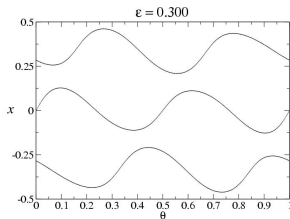
52

Unstable manifold ($\varepsilon = 0.5$)

Bundle merging causing breakdown

53

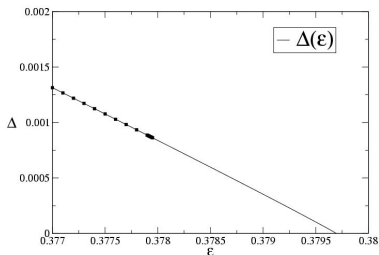
A 3-periodic torus close to breakdown, and projectivized bundles



Bundle merging causing breakdown

54

Quantitative estimates (universal laws)

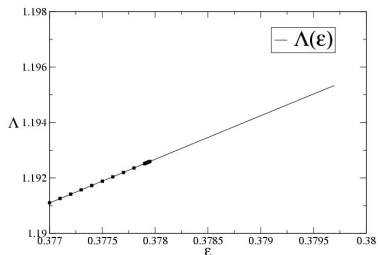


$$\Delta_\epsilon \sim \alpha(\epsilon_c - \epsilon)^\beta \text{ if } \epsilon \lesssim \epsilon_c$$

$$\epsilon_c = 0.3796965$$

$$\alpha = 0.4063$$

$$\beta = 0.9693 \approx 1$$



$$\Lambda_\epsilon \sim \Lambda_c + A(\epsilon_c - \epsilon)^B \text{ if } \epsilon \lesssim \epsilon_c$$

$$\Lambda_c = 1.19533$$

$$A = -1.6$$

$$B = 1.00 \approx 1$$

From the numerical experiments

55

The formation of a SNA in the linearized dynamics of a saddle type torus produces the sudden growth of the spectrum.

The torus is destroyed in such transition.

There are scaling relations in the observables (distance between bundles, Lyapunov multipliers), that are universal.

Validation of Numerical Computations

A Validation algorithm

57

From Newton-Kantorovich to the age of computers

Goal: Use computers to validate computations, proving existence and (local) uniqueness of fiberwise hyperbolic invariant tori.

We use an *a posteriori* theorem based on an adaptation of the Newton-Kantorovich theorem to the problem [HdL106].

The validation procedure is:

- Obtain initial data via some (non-rigorous) numerical method.
- Transform initial data to Fourier models.
(Fourier model = trigonometric polynomial with interval coefficients that encloses a continuous periodic function).
- Check hypothesis of the theorem using rigorous manipulation of the Fourier models.

A Validation algorithm

58

Step 0 of 5. Initial data

0.1.- Modelize with Fourier models:

- An approximate invariant torus $K: \mathbb{T}^d \rightarrow \mathbb{R}^n$.
- Two continuous matrix-valued maps $P_1, P_2: \mathbb{T}^d \rightarrow GL(n, \mathbb{R})$, where P_1 has in its columns an approximation of the invariant subbundles and P_2 is an approximate inverse of P_1 .
- A continuous block diagonal matrix-valued map $\Lambda: \mathbb{T}^d \rightarrow GL(n, \mathbb{R})$ which satisfies, approximately

$$P_2(\theta + \omega) D_z F(K(\theta), \theta) P_1(\theta) \simeq \Lambda(\theta) = \begin{pmatrix} \Lambda_{n_s}(\theta) & 0 \\ 0 & \Lambda_{n_u}(\theta) \end{pmatrix}.$$

Λ modelizes approximately the dynamics on the invariant subbundles.

A Validation algorithm

59

Step 1 of 5: Checking hyperbolicity

1.1.- Compute the upper bounds:

$$\|P_2(\theta + \omega)D_z F(K(\theta), \theta)P_1(\theta) - \Lambda(\theta)\|_\infty \leq \sigma$$

$$\|P_2(\theta)P_1(\theta) - \text{Id}\|_\infty \leq \tau$$

$$\max \{ \|\Lambda_{n_s}(\theta)\|_\infty, \|\Lambda_{n_u}(\theta)^{-1}\|_\infty \} \leq \lambda$$

1.2.- Check $\lambda + \sigma + \tau < 1$. If not, validation fails.

A Validation algorithm

60

Step 2 of 5: Checking approximate invariance

2.1.- Compute the upper bound:

$$\|P_2(\theta)(F(K(\theta - \omega), \theta - \omega) - K(\theta))\|_\infty \leq \rho$$

2.2.- Compute the upper bound:

$$\frac{\rho}{1 - (\lambda + \sigma + \tau)} \leq \varepsilon.$$

A Validation algorithm

61

Step 3 of 5: Checking Lipschitz condition

3.1.- Compute the upper bound:

$$\|P_2(\theta + \omega) D_z^2 F(z, \theta) [P_1(\theta) \cdot, P_1(\theta) \cdot]\|_\infty \leq b$$

for $\theta \in \mathbb{T}^d$ and $z \in B(K(\theta), 2(1 + \tau)\varepsilon)$.

3.2.- Compute the uppers bounds:

$$\frac{b}{1 - (\lambda + \sigma + \tau)} \leq \beta, \quad \beta\varepsilon \leq h.$$

A Validation algorithm

Step 4 of 5: Validation of torus

4.1.- If $h < \frac{1}{2}$ there exists an invariant torus $K_*: \mathbb{T}^d \rightarrow \mathbb{R}^n$ with

$$\|P_1(\theta)^{-1} (K_*(\theta) - K(\theta))\|_\infty < r_0$$

where

$$\frac{1 - \sqrt{1 - 2h}}{h} \cdot \varepsilon \leq r_0.$$

4.2.- This invariant torus is unique in the ball centered at the approximate invariant torus K_0 and radius

$$r_1 \leq \frac{1 + \sqrt{1 - 2h}}{h} \cdot \varepsilon.$$

A Validation algorithm

63

Step 5 of 5: Validation of invariant bundles

5.1.- Compute the upper bounds:

$$\|\Lambda(\theta)\|_\infty \leq \hat{\lambda},$$

$$\frac{\lambda}{1-\lambda^2} \frac{1}{1-\tau} \left(br_0 + \sigma + \hat{\lambda}\tau \right) \leq \mu.$$

5.2.- If $\mu < \frac{1}{4}$ then, there exist continuous matrix-valued maps $P_* : \mathbb{T}^d \rightarrow GL(n, \mathbb{R})$, and $\Lambda_* : \mathbb{T}^d \rightarrow GL(n, \mathbb{R})$ (block-diagonal), such that:

- $P_*(\theta + \omega)^{-1} D_z F(K_*(\theta), \theta) P_*(\theta) = \Lambda_*(\theta)$;
- $\|P_1(\theta)^{-1} (P_*(\theta) - P(\theta))\|_\infty \leq \frac{\mu}{\sqrt{1-4\mu}}$;
- $\|\Lambda_*(\theta) - \Lambda(\theta)\|_\infty \leq \frac{1}{1-\tau} \left(br_0 + \sigma + \hat{\lambda}\tau \right) \left(1 + \frac{\mu}{\sqrt{1-4\mu}} \right)$.

An example

64

A non-invertible quasiperiodically driven system

The **driven logistic map** is defined as the skew product

$$\begin{aligned} f: \mathbb{R} \times \mathbb{T} &\longrightarrow \mathbb{R} \times \mathbb{T} \\ (z, \theta) &\longrightarrow (a(1 + D \cos(2\pi\theta))z(1 - z), \theta + \omega) \end{aligned} \quad ,$$

where $\omega = \frac{\sqrt{5}-1}{2}$; and a and D are parameters.

In the following, we fix $D = 0.1$ and let a vary.

Numerical exploration: $D = 0.1$

65

The Heagy-Hammel route

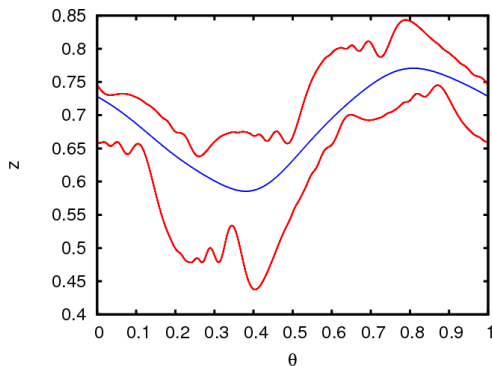


Figure: 2 period attracting curve for $a = 3.24$.

Numerical exploration: $D = 0.1$

65

The Heagy-Hammel route

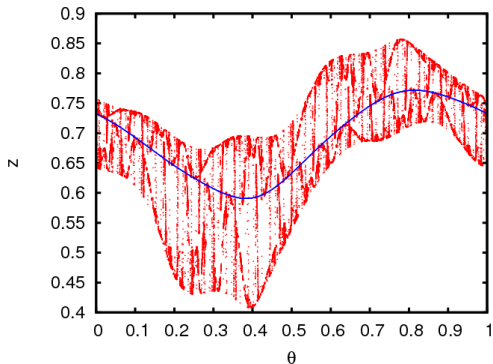


Figure: 2 period attracting set for $a = 3.272$.

Numerical exploration: $D = 0.1$

66

The Heagy-Hammel route

Numerical facts:

- There exists a repeller curve for all $a > 3.143$.
- There exists a 2 period attracting curve for $3.143 < a < 3.271383$. It's non reducible when $a > 3.17496$.

Validation of tori on the verge of breakdown

67

- We have validated the 2 period attracting curve for several values of $a \in [3.143, 3.269]$.
- Due to the non reducible nature of the tori, the slopes of some initial data are quite high. For example, at $a = 3.269$, the maximum slope of P_1 is $4.25 \cdot 10^6$.

Initial data to validate

Computing uniform attractiveness

68

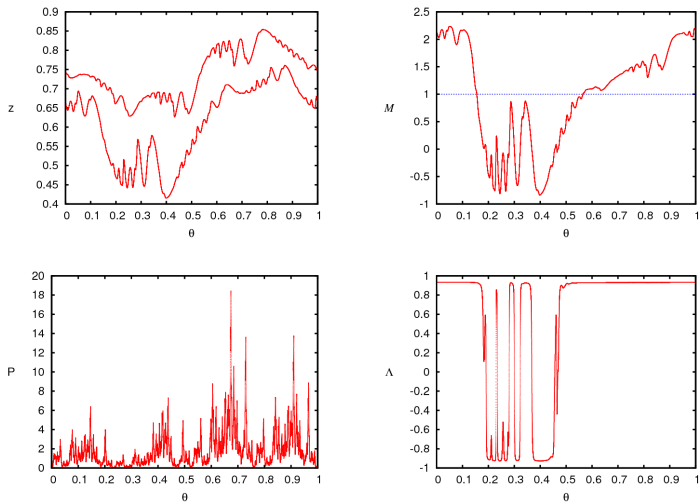


Figure: Initial data of the 2 period attracting torus with $a = 3.265$.

Initial data to validate

Computing uniform attractiveness

68

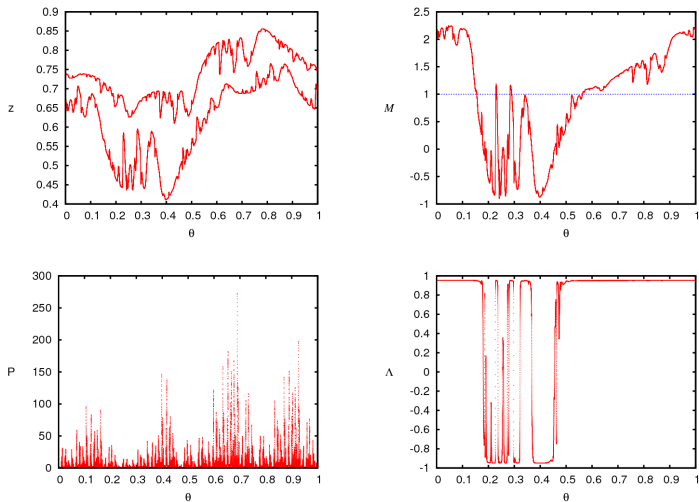


Figure: Initial data of the 2 period attracting torus with $a = 3.269$.

Validation results.

69

a	3.265	3.268	3.269
h	3.046383e-05	2.248226e-03	4.203495e-01
r_0	5.365990e-09	1.701127e-07	3.635973e-06
r_1	3.522752e-04	1.509902e-04	8.466295e-06
nodes	3000	17000	27000
Time comp. (min.)	5	130	361

Table: Validation results of the period 2 invariant torus of the driven logistic map for different values of the parameter a .

Summary

Conclusions

71

Problems, tools and applications

Problems: Computation of **invariant tori** and their **whiskers**

Tools:

- The **parameterization method**: to find equations for the invariant manifold and the dynamics on it.
- The equations are **functional equations**. We use **Newton**-like methods (for tori) and **normal form** methods (for whiskers) in suitable spaces of functions.
- These equations are discretized in terms of Fourier or Fourier-Taylor series. We use **Fourier Transform (FT)** and **Automatic Differentiation (AD)**.

Applications:

- Phenomena at the **breakdown of dichotomies**.
- **Resonances** in Hamiltonian elliptic tori.
- **Computer assisted proofs** on the verge of breakdown.

Work in progress/Future work

72

To do list

- Applications to some problems in Celestial mechanics
- Higher dimensional tori, sparse Fourier series
- Higher dimensional models
- Quasi-periodic solutions in some PDE's
- Quasi-periodic solutions in some delay equations
- More general normally hyperbolic manifolds
- A better connection with KAM theory
- Better theory for elliptic Hamiltonian tori
- Computer assisted proofs
- ...

Bibliography

Sources of this lecture

- A.H., R. de la Llave, "A parameterization method for the computation of invariant tori and their whiskers in quasi-periodic maps: "
 - 1 Rigorous results.
 - 2 Numerical Algorithms.
 - 3 Explorations and Mechanisms for the Breakdown of Hyperbolicity.
- A.H., R. de la Llave, "Manifolds on the verge of a hyperbolicity breakdown"
- A.H, R. de la Llave, "Spectral Theory and Dynamical Systems" (book in preparation)
- J.-Ll. Figueras-Romero, A. H., "Reliable computation of robust response tori" (preprint)
- J.-Ll Figueras-Romero (phd. thesis)

Epitaph

74

From Theorems to Algorithms.
From Algorithms to Numerics.
From Numerics to Experiments.
From Experiments to Conjectures.
From Conjectures to Theorems?